Arch Virol (2014) 159:1403–1412
DOI 10.1007/s00705-013-1962-6

ORIGINAL ARTICLE

Pathological and microbiological findings from mortality of the Chinese giant salamander (*Andrias davidianus*)

Yan Meng · Jie Ma · Nan Jiang · Ling-Bing Zeng · Han-Bing Xiao

Received: 9 August 2013 / Accepted: 22 November 2013 / Published online: 3 January 2014

Abstract The Chinese giant salamander, *Andrias davidianus*, is a nationally protected and cultured species in China. Recently, a severe epizootic occurred in cultured Chinese giant salamanders in Hubei, Hunan, Sichuan, Shaanxi, and Zhejiang provinces of China, causing substantial economic losses. The typical clinical signs of diseased larval animals were jaw and abdominal swelling and subcutaneous hemorrhaging. Diseased adult animals exhibited skin hemorrhages, ulceration of the hind limbs, and multiple hemorrhagic spots in the visceral organs. Histopathological observation indicated tissue necrosis and cytoplasmic inclusions in the spleen, liver and kidney, suggestive of viral disease. A viral agent was isolated from affected tissues in cell culture. The virus was determined to be pathogenic after experimental infection. Electron microscopy revealed iridovirus-like virions with a size of 140-180 nm in diameter inside the kidney of naturally infected animals and in cell culture. The major capsid protein (MCP) of the virus exhibited 98-99 % sequence identity to ranaviruses. Additionally, phylogenetic analysis indicated that the virus belonged to the genus *Ranavirus*. Comparative analysis of the MCP gene sequence with those of other viruses previously isolated from Chinese giant salamanders revealed that these isolates were highly similar, although a few variations were observed. The virus was preliminarily named Chinese giant salamander iridovirus (GSIV).

Y. Meng · J. Ma · N. Jiang · L.-B. Zeng (✉) · H.-B. Xiao
Yangtze River Fisheries Research Institute, Chinese Academy of Fishery Sciences, Wuhan 430223, Hubei, China
e-mail: zenglingbing@gmail.com

Y. Meng
Freshwater Fisheries Research Center, Chinese Academy of Fishery Sciences, Wuxi 214081, Jiangsu, China

Introduction

The Chinese giant salamander, *Andrias davidianus*, belonging to the family *Cryptobranchidae*, is the largest extant amphibian species in the world. Besides its value as a food source and in medicine, it is valued for research on animal evolution, biodiversity, and molecular mechanism(s) of sex determination based on its unique phylogenetic position and physiological features [1]. However, the Chinese giant salamander population has declined sharply in the past 50 years due to the synergistic effects caused by habitat deterioration, environmental pollution, climate change, infectious diseases, and commercial trade [2, 3]. This endangered amphibian has been under state protection since 1973 and is currently listed in annex I of the Convention on International Trade in Endangered Species of Wild Fauna and Flora (CITES) and as class II on the national list of protected animals in China [3]. In China, Chinese giant salamander farming has grown rapidly within the last decade. Each year, approximately two million Chinese giant salamanders are bred in China. Due to the growing interest in culturing this species, development of intensive farming techniques, and frequent trading, emerging viral infectious diseases have been increasing. These diseases appear to affect both larvae and adult Chinese giant salamanders, resulting in hemorrhages, ascites, skin diseases and pneumonitis. The economic consequences of these diseases are serious.

Members of the family *Iridoviridae* are large DNA viruses with double-stranded DNA genomes ranging from 140 to 303 kb and icosahedral capsids of 120-350 nm in diameter. These pathogens have caused a number of serious systemic diseases in both wild and cultured aquatic animals [4–7]. Five genera of *Iridoviridae* are currently recognized, including *Megalocytivirus*, *Chloriridovirus*,

Lymphocystivirus, *Iridovirus* and *Ranavirus*. Members of the genus *Ranavirus* have been reported to be associated with several outbreaks in amphibians. About twenty viruses belonging to the genus *Ranavirus* can infect amphibians worldwide. For example, a ranavirus has been confirmed as the cause of an epizootic in juvenile and adult tiger salamanders (*Ambystoma tigrinum diaboli*) [8]. Majji *et al.* [9] described an iridovirus that caused disease in American bullfrogs (*Rana castesbeiana*) and reported an outbreak of ranavirus infection in a group of juvenile Hermann's tortoises (*T. hermanni*) in the United States [10]. In China, a ranavirus was first isolated from red-legged frog tadpoles (*Rana auroa*) [11]. Subsequently, this ranavirus was isolated from *Rana grylio* [12] and *Rana tigrina rugulosa* [13]. As an emerging pathogen affecting the Chinese giant salamander, Geng *et al.* [14] first reported a ranavirus associated with morbidity and mortality in farmed Chinese giant salamanders. This iridovirus was also reported in 2010 [15, 16]. But in these reports, the viruses were all isolated from the city of Hanzhong or the neighboring city of Hanzhong, Shannxi Province, and identified as members of the genus *Ranavirus* or the family *Iridoviridae*.

Here, we report the isolation and identification of a virus causing hemorrhagic disease in Chinese giant salamanders in Hubei Province in November 2010. Infections led to systemic disease. The pathological changes included scattered areas of single-cell necrosis, variably sized areas of focal necrosis, and cytoplasmic inclusions in disease tissues. Electron microscopy suggested that an iridovirus-like agent was present in the infected cells. Based on experimental infection test, cell culture, and analysis of the major caspid protein (MCP) gene, the virus was confirmed to be a ranavirus. Comparative analysis of this ranavirus with iridoviruses previously isolated from the Chinese giant salamander revealed that they were highly similar, although a few variations were observed.

Materials and methods

Animals and cell line

Diseased Chinese giant salamanders were collected from a farm in the city of Jingzhou, Hubei Province, in November, 2010. Healthy Chinese giant salamanders were obtained from the Yangtze River Fisheries Research Institute, Chinese Academy of Fishery Sciences (CAFS) in Jingzhou, Hubei Province. The healthy salamanders were supplied with tap water at 16±2 °C and were tested to be free of iridovirus before the experiment. The *epithelioma papilloma cyprinid* (EPC) cell line [17] was obtained from the China Center for Type Culture Collection (CCTCC), Wuhan University. The cells were incubated at 25 °C and grown in minimum essential medium (MEM, Sigma) supplemented with 10 % fetal bovine serum, 100 IU/ml penicillin, and 40 μg/ml streptomycin.

Histopathology

Spleens, kidneys, and livers from ten affected Chinese giant salamanders were fixed in 4 % paraformaldehyde (PFA) at 4 °C. Fixed samples were washed with phosphate-buffered saline (PBS), dehydrated with 30 % sucrose/PBS, and embedded in optimum cutting temperature compound (OCT, Leica, Germany). Samples were sectioned (8 μm) at −20 °C and stained with haematoxylin and eosin (HE) using standard procedures.

Viral isolation

Spleens, livers and kidneys obtained from diseased Chinese giant salamanders were homogenized in sterile PBS (pH 7.2, Sigma) at a ratio of 1:10 (w/v) on ice. After triplicate freeze-thaws, the homogenate was centrifuged at 5000×g for 30 min, and the supernatant was collected and filtered through a 0.22-μm filter (Nalgene, USA). One ml of the filtered homogenate was added to 10 μg polybrene and inoculated onto EPC cells in a 25-cm^2 flask (Corning, USA). After 1 h adsorption at 25 °C, the homogenate was aspirated and 5 ml MEM containing 2 % fetal bovine serum (FBS, Gibco) was added to the flask. The cells were incubated at 25 °C and observed for cytopathic effect (CPE). Titration of the virus isolated was done on EPC cells in a 96-well microculture plate (Corning, USA). The viral suspension was serially diluted from 10^{-1} to 10^{-9} in MEM. Each dilution was inoculated into eight wells with 0.1 ml per well and incubated at 25 °C. The viral titer was expressed as the 50 % tissue culture infective dose (TCID50) by the method of Reed and Muench [18].

Electron microscopy

Tissue samples and EPC cells infected with the virus were used for electron microscopy. The procedure was described previously [19]. Briefly, the samples were fixed in 2.5 % cold glutaraldehyde and then were dehydrated and embedded for ultra-thin sectioning (Leica UC7, Germany). The sections were stained with uranyl acetate and examined by electron microscopy and photographed (Tecnai, FEI EM, USA).

Experimental infection

Sixty healthy one-year-old Chinese giant salamanders (15-18 cm in length) were fed specific-pathogen-free fish meal

for six weeks prior to the initiation of the experiment. The Chinese giant salamanders were divided into two groups with thirty animals in each group. Each animal in one group was injected intraperitoneally with 0.2 ml of virus grown in cell culture (equivalent to 2×10^8 TCID50), and the control group was injected intraperitoneally with 0.2 ml of PBS (Sigma, USA). The salamanders were monitored daily for signs of infection and mortality. Deceased Chinese giant salamanders were collected and stored at −80 °C.

MCP gene cloning, sequencing, and sequence analysis

The sequences of the primers used for amplifying the entire MCP gene from the isolated virus were chosen from the conserved regions of iridovirus MCP genes in the GenBank database. The primer sequences are as follows: PH1, 5'-GTGGCAAACGGACACTTCAT-3'; PH2, 5'-ATAAT AAAAAGGAAATGTCT-3'. Primers were synthesized at Sangon BioTechnologies (Shanghai, China). The tissue homogenates from naturally diseased animals and experimentally infected animals as well as virus-infected EPC cells were used for viral genomic DNA extraction (DNA extraction kit, QIAGEN, Austria). The PCR reaction was conducted using the PCR Core System II (Promega, USA). The PCR reaction consisted of 5.0 μl of 10× reaction buffer, 0.4 μl of 10 μM dNTPs, 2.0 units of *Taq* DNA polymerase, 2.0 μl of 10 μM each primer, and 1 μg of the DNA template for a total reaction volume of 50 μl. PCR reactions were programmed for an initial denaturation step at 94 °C for 3 min, followed by 35 cycles of denaturation at 94 °C for 45 s, annealing at 56 °C for 30 s and extension at 72 °C for 90 s, and a final extension step at 72 °C for 10 min. The amplified products were detected via 1.5 % agarose gel electrophoresis. PCR products were purified using a PCR purification kit (OMEGA, USA). The purified products were cloned into the PMD18-T vector (Takara, Dalian, China) and sequenced at Shanghai GeneCore BioTechnologies Co., Ltd. (Shanghai, China).

The MCP sequence was submitted to GenBank (accession number, JN615141). The MCP sequence was searched in the GenBank database using the NCBI BLAST tool to identify highly similar viral sequences. The sequence alignment of the MCP gene was conducted using Mega 5.0 software (http://www.megasoftware.net/). The aligned sequences included Chinese giant salamander virus (CGSV, HQ684746), European sheatfish virus (ESV, FJ358609), frog virus 3 (FV3, FJ459783), epizootic haematopoietic necrosis virus (EHNV, AY187045.1), Bohle iridovirus (BIV, FJ358613), infectious spleen and kidney necrosis virus (ISKNV, HQ317465.1), ADIV isolated from Chinese giant salamander (KC465189.2), GSIV (isolated in this study, JN615141.1), a Chinese giant salamander virus isolate from Guizhou Province (GZ, KC816423.1), a Chinese giant salamander virus isolate from LveYang, Shannxi Province in 2011 (LY, KF023635.1), common midwife toad virus (CMTV, AFA44920), *Ambystoma tigrinum* virus (ATV, YP003785.1), soft-shelled turtle iridovirus (STIV, ACF42314) and lymphocystis disease virus (LCDV, GU939626.2). The alignment was input into MEGA 5.0 for phylogenetic analysis using the unweighted pair group method with arithmetic mean (UPGMA) method. Members of the genera *Lymphocystivirus* and *Megalocytivirus* were used as out-groups in the phylogenetic analysis. The amino acid sequences were aligned using MEGA 5.0.

Results

Symptoms

The diseased larvae were about three months old, 5-7 cm in length, and 3-5 g in weight. They were being farmed in plastic aquariums with tap water in a basement and fed with frozen chironomid larvae. Three hundred larval Chinese giant salamanders died within one month. The symptoms included swollen head and neck and subcutaneous hemorrhages on the dorsal and ventral surfaces (Fig. 1A). Diseased adult Chinese giant salamanders were found from September to October 2010 in Jingzhou at another farm. The adult animals displayed skin hemorrhages, swelling, and ulceration of the limbs (Fig. 1B). Dissection revealed that ascites filled the abdominal cavity, the stomach was pale and empty, and the intestine contained yellow mucus and was hemorrhagic. The spleen was fragile and had hemorrhagic spots. The kidney was also hemorrhagic.

Histopathology

Microscopic lesions were observed in the spleen, liver, and kidney tissues. Lesions consisted of scattered areas of single-cell necrosis and variably sized areas of focal necrosis. In the affected tissues, necrotic cells and cells adjacent to the areas of necrosis commonly contained cytoplasmic inclusions that stained basophilic to amphophilic using HE staining. Hyperplastic lymphoid nodules, splenocyte necrosis, and vacuolar degeneration were detected in the spleen. In addition, macrophages, nuclear debris, and cytoplasmic inclusions were observed in the lymphoid nodules. Many splenocytes had enlarged, pale-staining, enlarged hypochromatic nuclei with condensed chromatin, and irregularly shaped vacuoles. Vacuolar degeneration was observed in the spleen (Fig. 2A). Unaffected splenocytes were stained evenly and had no obvious lymphoid nodules (Fig. 2A′). Vacuolar degeneration and necrosis of renal hematopoietic tissue cells and glomeruli were detected in the renal tissues, which exhibited nuclear

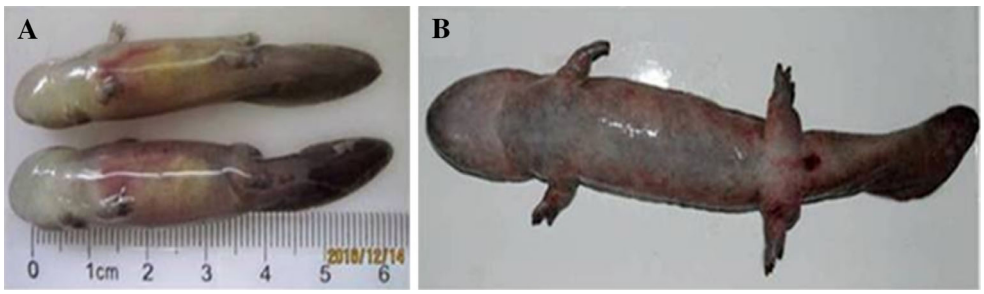

Fig. 1 Symptoms of diseased Chinese giant salamanders. **A** Chinese giant salamander larvae with swollen heads and necks and subcutaneous hemorrhage on the ventral surfaces, **B** adult animal with skin hemorrhages and swollen and ulcerated limbs

changes similar to the affected splenocytes. Cells of the glomerulus and hematopoietic tissue cells also frequently contained numerous cytoplasmic inclusions, which were either associated with single degenerating cells or large areas of focal necrosis. Nuclear debris was also detected in the renal tissues (Fig. 2B). The unaffected hematopoietic tissue cells and glomerulus cells were stained evenly without necrosis (Fig. 2B′). Liver sinusoids were hypertrophied and contained numerous macrophages. Hepatocytes also contained viral inclusions and nuclear debris, and the nuclear changes in necrotic hepatocytes were similar to those observed in affected splenocytes (Fig. 2C). Unaffected hepatocytes were stained evenly and exhibited a regular cell shape (Fig. 2C′).

Viral isolation and electron microscopy

Tissue homogenates from diseased animals were inoculated onto EPC cells and passaged. Cytopathic effects (CPE) in EPC cells were observed at 2 days postinfection. The infected EPC cells became refractile and exhibited cytoplasmic granules before dying. Small holes in the cell monolayer appeared and increased in size over time. The tissue culture infectious dose ($TCID_{50}$) was determined in a microplate culture system, and the viral titer ($TCID_{50}$ ml^{-1}) reached $10^{9.5-10.5}$. Electron microscopy also indicated that the EPC cells were infected with the virus.

Tissue samples from the liver, spleen, and kidney from diseased animals were observed by electron microscopy. In the kidney tissue, typical virus-like particles were observed in renal cells (Fig. 3). Many virus-like particles existed in cytoplasmic areas and appeared hexagonal or round. These virus-like particles were also observed in spleen and liver tissues. The particles were hexagonal and measured ~140 nm in diameter, and diagonally were approximately 180 nm. Typical iridovirus morphology was observed. Some virions accumulated in the cytoplasm, but others were free. On the edge of the cell membrane, a virion was observed budding and becoming larger (Fig. 4). Electron microscopy of thin sections revealed that there were abundant enveloped viruses appearing in the extracellular area, and non-enveloped virus particles appeared in the cytoplasm.

Experimental infections

Five days post-infection, the artificially infected Chinese giant salamanders began to show disease signs similar to those of naturally infected animals. The experimental infection results indicate that the mortality in the infected group exceeded 87 % at 10 days postinfection, while the control group remained normal (Table 1). The virus was isolated from the experimentally infected animals. Viral MCP gene assays demonstrated that the disease was caused by the viral infection.

Molecular identification and comparison based on the MCP gene

Based on PCR and sequencing, the MCP gene of the isolated virus was determined to be 1392 bp long. BLAST searches in the GenBank nr database showed that the cloned MCP gene was >98 % identical to the MCP sequences of ranaviruses isolated from other species, including FV3, EHNV and CGSV. Selected MCP sequences were used to construct a phylogenetic tree using the UPGMA method in MEGA 5.0 software. All selected sequences were clustered into three groups, belonging to the genera *Lymphocystivirus*, *Megalocytivirus* and *Ranavirus*, respectively. The Chinese giant salamander iridovirus was clustered in the ranavirus clade (Fig. 5). The virus was given the name Chinese giant salamander iridovirus (GSIV). There were five MCP sequences of iridovirus isolated from Chinese giant salamander in the GenBank database. They were CGSV (HQ684746.2), ADIV (KC465189.2), GSIV (isolated in this study, JN615141.1), a Chinese giant salamander virus isolate from Guizhou Province (GZ, KC816423.1), and a Chinese giant salamander virus isolate from LveYang, Shannxi Province, in

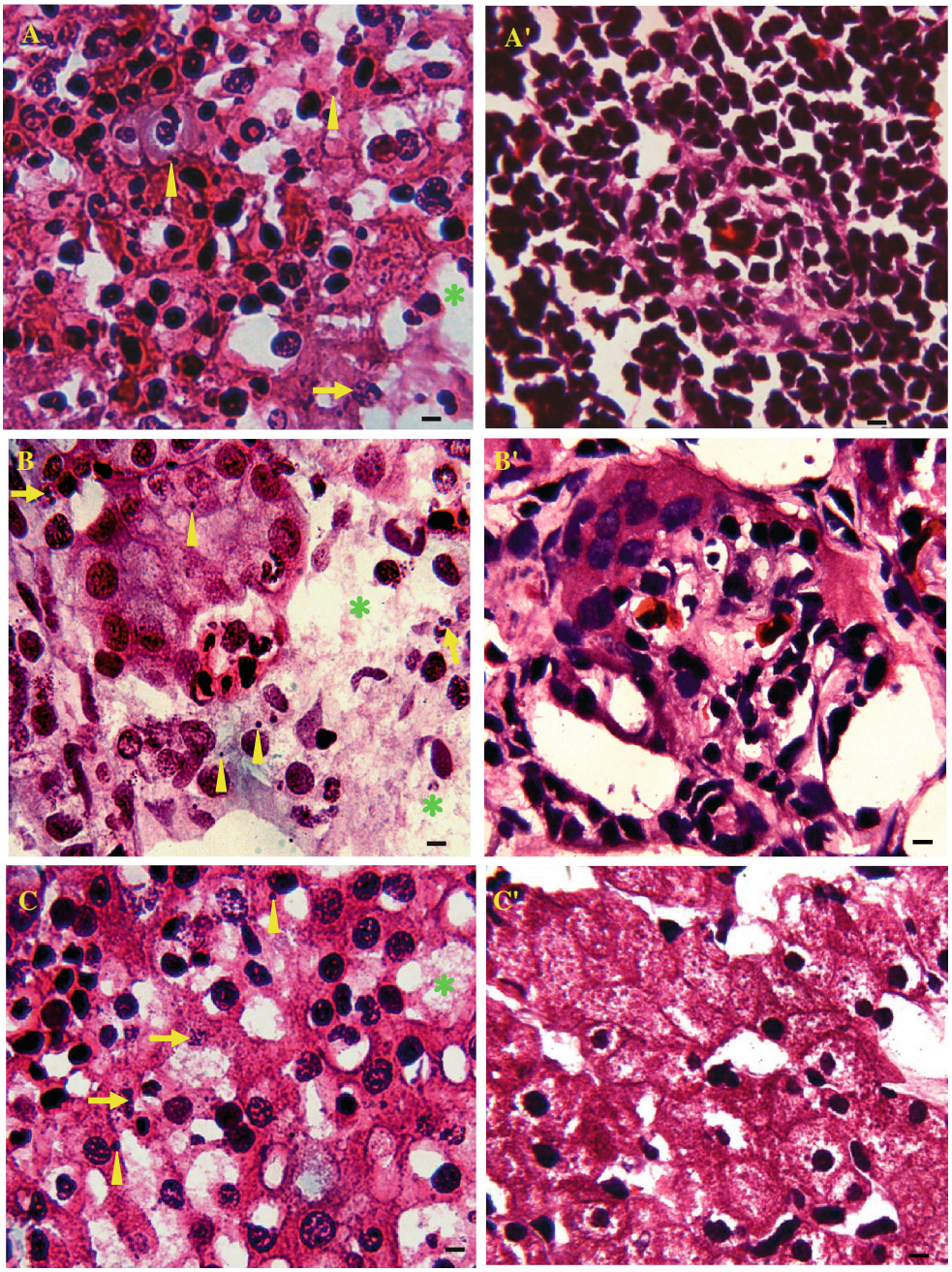

Fig. 2 Histopathologic sections of infected organs. **A** Spleen. Cytoplasmic inclusions (yellow arrowhead), nuclear debris (yellow arrow), and vacuolar degeneration (green asterisk) of splenocytes. **B** Kindey. Cytoplasmic inclusions (yellow arrowhead), nuclear debris (yellow arrow), and vacuolar degeneration (green asterisk) of renal hematopoietic tissue cells and glomerulus cells. **C** Liver. Cytoplasmic inclusions (yellow arrowhead), nuclear debris (yellow arrow), and macrophages (green asterisk) of hepatocytes. **A'**, **B'** and **C'** are normal tissues. Scale bars (black line) =20μm

2011 (LY, KF023635.1). The amino acid sequence of GSIV was aligned with them and other ranaviruses from the GenBank database. The results indicated that the isolates from Chinese giant salamanders were more similar to each other than to other ranaviruses (Fig. 6). In the five sequences of isolates from Chinese giant salamanders, there were only four variations.

Discussion

Amphibian population decline is one of the most critical threats to global biodiversity. While habitat destruction is clearly the most important factor causing population declines, viral and fungal infections have caused several serious amphibian population declines [20]. The Chinese

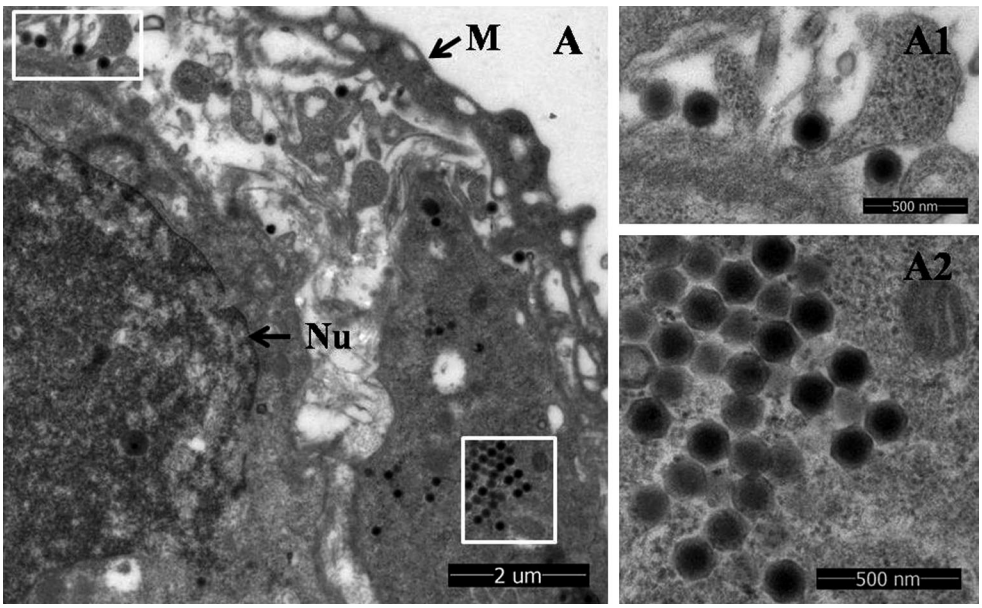

Fig. 3 Electron micrograph of iridovirus-like particles in the kidney of a diseased Chinese giant salamander. **A** virus-like particles were observed in the kidney of diseased animals; **A1**, virus in the renal tubular epithelium cells with a hexagonal shape; **A2**, typical iridovirus-like particle with icosahedral morphology. Nu, nucleus; M, membrane. **A1** and **A2** correspond to the areas within the white rectangles in **A**, shown at higher magnification

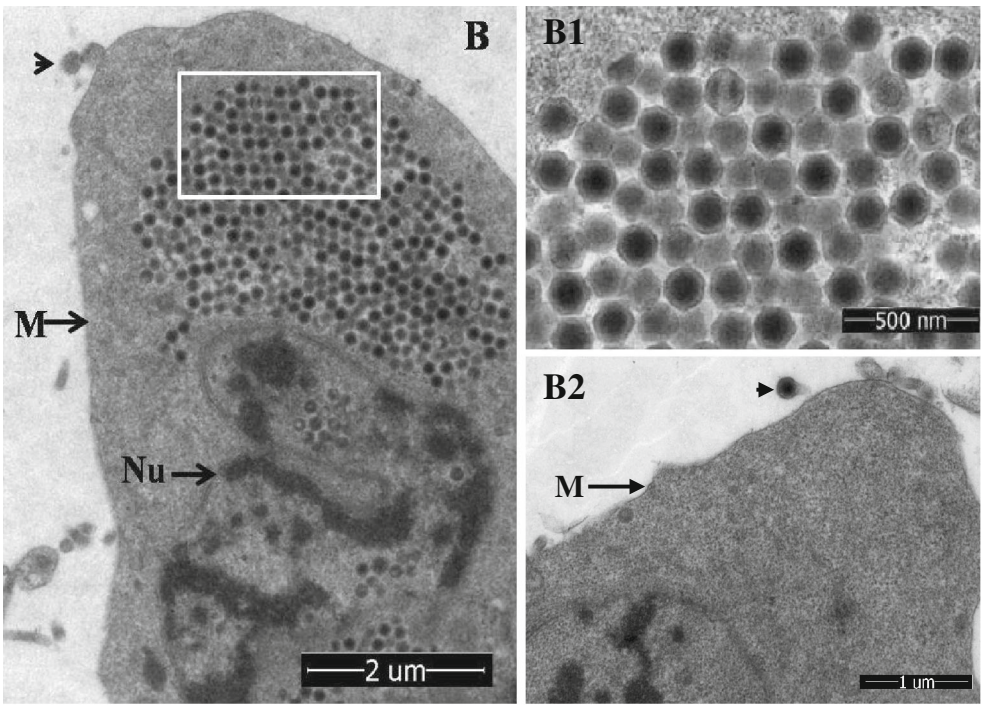

Fig. 4 Electron micrograph of isolated iridovirus-infected EPC cells. **B**, virus assembled in the cytoplasm and the broken nucleus zone; **B1**, iridovirus-like particles in crystalline arrays in the cytoplasm; **B2**, a virion is budding through the cell membrane to acquire an envelope (arrowhead). Nu, nucleus; M, membrane. **B1** corresponds to the area within the white rectangle in **B**, shown at higher magnification

giant salamander is the largest amphibian species in the world, growing up to 1.8 meters, and can live for over 50 years. This species is classified as critically endangered in the IUCN Red List because more than 80 % of the wild population has disappeared since the 1960s [3]. Artificial propagation has been developed for the Chinese giant

Table 1 Results of experimental infections

Treatment	Dose (ml/individual)	Number (individuals)	Death count (individuals)	Mortality
Virus suspension	$0.2/2 \times 10^8$ TCID50	30	26	87 %
DPBS	0.2	30	0	0

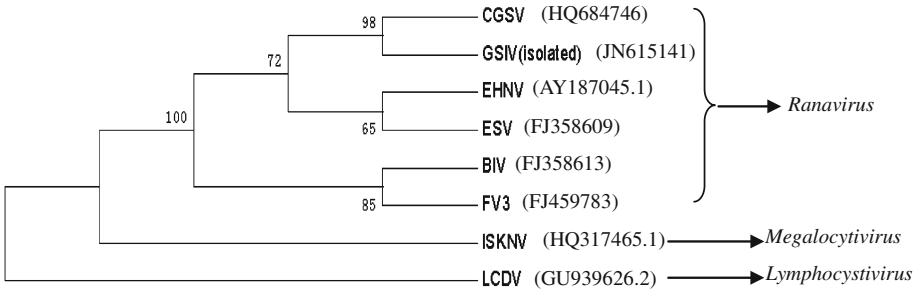

Fig. 5 Phylogenetic organization of GSIV isolated in this study and other ranaviruses. Numbers at the nodes are bootstrap values. The GenBank accession numbers are shown in parentheses

salamander; however, disease is a great concern with respect to preservation of the species.

Ranaviruses have been isolated from aquatic vertebrates at different taxonomic levels and developmental stages, and they exhibit differing host specificity [21–24]. Ranaviruses are capable of infecting amphibians from at least 14 families and over 70 different species. In amphibians, ranaviruses have been confirmed to infect juvenile, metamorphosing, and metamorphosed animals [20]. Tiger salamanders [8], water frogs [25], and Chinese giant salamanders have been affected at different life stages. Most often, infections are systemic, causing severe necrosis of multiple tissues including the hematopoietic tissue, liver, kidney, digestive tract, and skin [26, 27]. Cytoplasmic inclusion bodies were associated with small foci of necrosis in these involved tissues of Chinese giant salamanders. Pycnotic cell nuclei were also observed. It is obvious that these organs were the targets of viral infection and displayed a wide range of necrosis. These lesions were similar to those observed in other ranavirus-associated diseases, such as infections in juvenile and adult tiger salamanders in southern Saskatchewan, Canada [8], and water frogs [25]. Ranavirus infections also cause symptoms such as erythema, ulceration, and subcutaneous edema [8, 28, 29]. In Chinese giant salamanders, dermal ulcerations and subcutaneous edema are the predominant manifestations with systemic hemorrhages. The symptoms and histopathological observations of infected Chinese giant salamanders in this study were consistent with the descriptions above, suggesting that the infection was likely caused by ranaviruses.

Confirming a ranavirus infection can be done via electron microscopy, viral isolation in susceptible cell lines, nucleotide-based molecular identification, and immunological and serological assays [30]. Identification of ranavirus in tissue sections is also helpful in understanding amphibian viral diseases [31]. In this study, lesioned tissues and infected EPC cells were used to detect the virus by electron microscopy. The results revealed that virions had an icosahedral capsid with a diameter of approximately 140 nm. Viral assembly occurred in the cytoplasm, which is a characteristic of members of the family *Iridoviridae*. Virions accumulated into clusters in the cytoplasm with the potential to acquire an envelope via budding through the plasma membrane. A seminal report by Goorha *et al.* about frog virus 3 DNA replication described a similar process [32]. The highly conserved MCP is the main structural component of iridoviruses. Previous studies have suggested that the MCP gene is an appropriate marker to distinguish different iridovirus strains and species [8, 33, 34]. The complete MCP gene of the isolated virus exhibited 98-99 % sequence identity to published ranavirus sequences. Meanwhile, phylogenetic analysis grouped the isolated Chinese giant salamander iridovirus into the ranavirus clade. All of these results support that this Chinese giant salamander iridovirus belongs to the genus *Ranavirus*.

As an emerging disease of the Chinese giant salamander, the pathogen has been described as a ranavirus or an iridovirus in previous reports [14–16]. In the three published papers, the agent virus, ranavirus or iridovirus, was likely the same virus. The samples were collected from Shanxi Province, China. In addition, these viral strains shared similar epidemic timing, from February to October 2010. In this study, GSIV was isolated in December 2010 and was associated with two main disease syndromes: animals were noted either as having skin ulceration with necrosis of distal limbs or as having systemic haemorrhages. The slight differences in MCP suggest that these isolates are different iridovirus strains of the same species [35]. Five MCP sequences were extracted from the

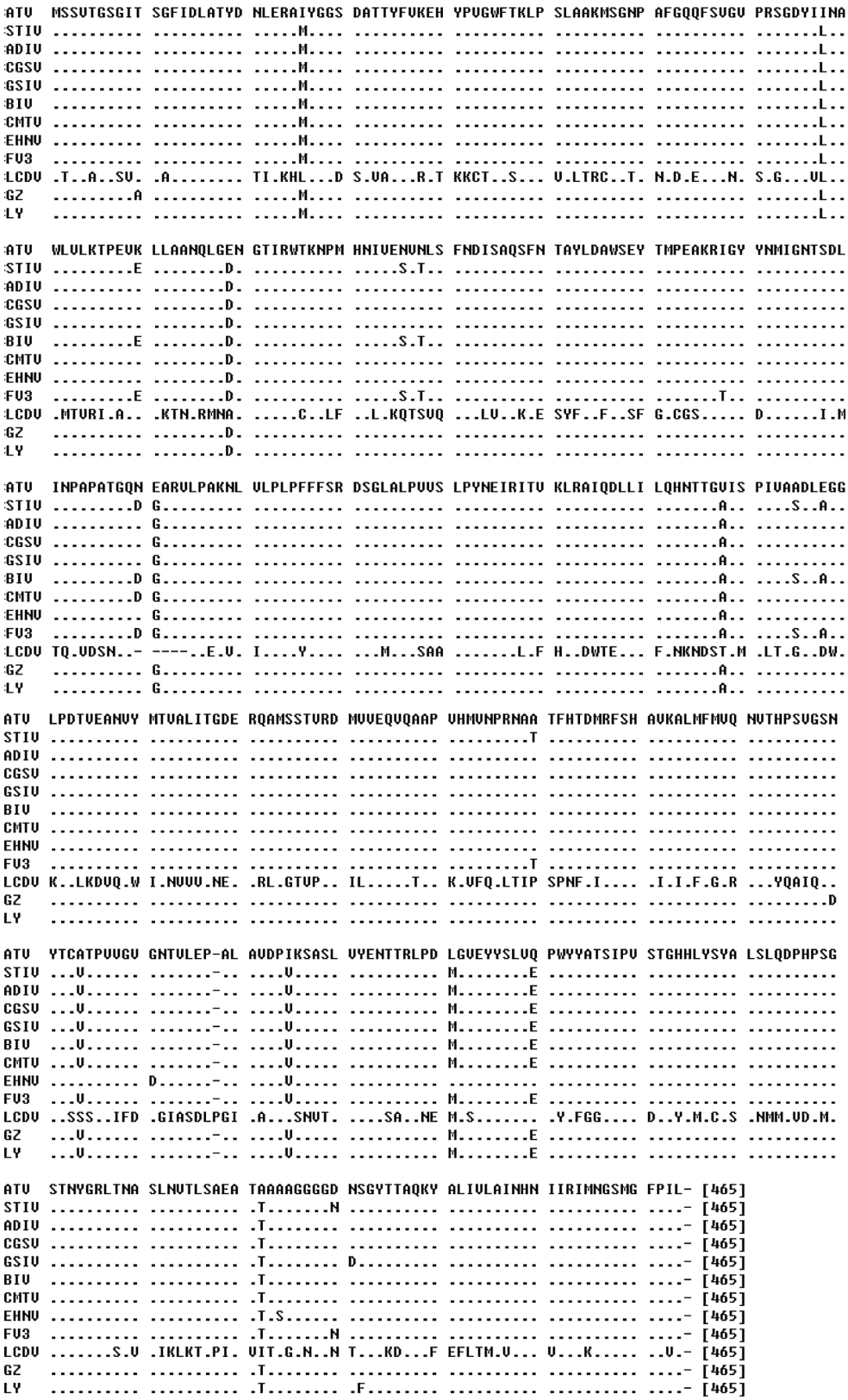

Fig. 6 Alignment of deduced amino acid sequences of ranaviruses MCP genes isolated from different species

GenBank database, including the iridoviruses CGSV (HQ684746.2), ADIV (KC465189.2), GSIV (isolated in this study, JN615141.1), a Chinese giant salamander virus isolate from Guizhou Province (KC816423.1) and a Chinese giant salamander virus isolate from Shanxi Province (KF023635.1). The nucleotide sequence length of GCSV

(1453 bp) is longer than that of the other four sequences (1392 bp). Comparison of these sequences showed that they exhibited 98-99 % similarity, though there were a number of variations. Alignment of amino acid sequences of MCP further supports that the strain in our study may have the same origin as other strains previously isolated from Chinese giant salamanders (Figures 5 and 6). We speculate that these strains originated from a common ranavirus and have been circulating in China to cause outbreaks. The host immune pressure and other factors may drive the diversity and variations that were observed in the gene and amino acid sequences. Genetic variations may contribute to virulence, pathogenesis, and host adaptation of viral pathogens. However, it is not clear whether a specific genotype is linked to increased virulence, because only a few ranavirus strains have been identified and characterized so far. No significant difference in clinical manifestations was observed, and thus, these minor genetic variations may not contribute directly to virulence. In summary, we have isolated an iridovirus strain that caused infections of Chinese giant salamanders, and this strain is closely related to other iridovirus strains previously identified in China.

In this study, GSIV was isolated from a Chinese giant salamander in Hubei Province. Although it was similar to previously identified viruses [14–16], there were some differences among them. To further investigate the genetic variation and population dynamics of these iridovirus strains, large-scale studies on epidemiological surveillance, genome sequencing, and population genomics are necessary, which will ultimately be useful for the prevention and control of this disease.

Acknowledgements The authors would like to thank Dr. Jie Huang, Yellow Sea Fisheries Research Institute, Chinese Academy of Fishery Sciences, for help with histopathology. This work was supported by the Special Fund for Agro-Scientific Research in the Public Interest (201203086) and the National Nonprofit Institute Research Grant of Freshwater Fisheries Research Center, Chinese Academy of Fishery Sciences (2013JBFZ02).

References

1. Hou JH, Zhu BC, Dong YW, Li PQ, Liu HM, Wan XQ (2004) Research advances of Chinese giant salamander, *Andrias davidianus*. Sichuan J Zool 22:262–267
2. Wang XM, Zhang KJ, Wang ZH, Ding YZ, Wu W, Huang S (2004) The decline of the Chinese giant salamander *Andrias davidianus* and implications for its conservation. Oryx 38:197–202
3. Zhang KJ, Wang XM, Wu W, Wang ZH, Huang S (2002) Advances in conservation biology of Chinese giant salamander. Biodiversity Sci 10:291–297
4. Hyatt AD, Williamson M, Coupar BEH, Middleton D, Hengstberger SG, Gould AR, Selleck P, Wise TG, Kattenbelt J, Cunningham AA, Lee J (2002) First identification of a ranavirus from green pythons (*Chondropython viridis*). J Wildl Dis 38:239–252
5. Lu L, Zhou SY, Chen C, Weng SP, Chan SM, He JG (2005) Complete genome sequence analysis of an iridovirus isolated from the orange-spotted grouper, *Epinephelus coioides*. Virology 339:81–100. doi:10.1016/j.virol.2005.05.021
6. Wang Q, Zeng WW, Li KB, Chang OQ, Liu C, Wu GH, Shi CB, Wu SQ (2011) Outbreaks of an iridovirus in marbled sleepy goby, *Oxyeleotris marmoratus* (Bleeker), cultured in southern China. J Fish Dis 34:399–402. doi:10.1111/j.1365-2761.2011.01244.x
7. Whittington RJ, Becker JA, Dennis MM (2010) Iridovirus infections in finfish-critical review with emphasis on ranaviruses. J Fish Dis 33:95–122. doi:10.1111/j.1365-2761.2009.01110.x
8. Bollinger TK, Mao JH, Schock D, Brigham RM, Gregory V (1999) Pathology, isolated and preliminary molecular characterization of a novel iridovirus from tiger salamander in Saskatchewan. J Wildl Dis 35:413–429
9. Majji S, LaPatra S, Long SM, Sample R, Locke B, Sinning A, Chinchar VG (2006) *Rana catesbeiana* virus Z (RCV-Z), a novel pathogenic strain of frog virus 3. Dis Aquat Org 73:1–11. doi:10.3354/dao073001
10. Marschang RE, Becher P, Posthaus H, Wild P, Thiel HJ, Doblies UM, Kaleta EF, Bacciarini LN (1999) Isolation and characterization of an iridovirus from Hermann's tortoises (*Testudo hermanni*). Arch Virol 144:1909–1922. doi:10.1007/s007050050714
11. Mao JH, Green DE, Fellers G, Chinchar VG (1999) Molecular characterization of iridoviruses isolated from sympatric amphibians and fish. Virus Res 63:45–52. doi:10.1016/S0168-1702
12. Zhang QY, Xiao F, Li ZQ, Gui JF, Mao JH (2001) Characterization of an iridovirus from the cultured pig frog (*Rana frylio*) with lethal syndrome. Dis Aquat Org 48:27–36
13. He JG, Lu L, Deng M, He HH, Weng SP, Wang XH, Zhou SY, Long QX, Wang XZ (2002) Sequence analysis of the complete genome of an iridovirus isolated from the tiger frog. Virology 292:185–197. doi:10.1006/viro.2001.1245
14. Geng Y, Wang KY, Zhou ZY, Li CW (2011) First report of a Ranavirus associated with morbidity and mortality in farmed Chinese giant salamanders (*Andrias davidianus*). J Comp Path 145:95–102 10.1016/j.jcpa.2010.11.012
15. Dong W, Zhang X, An J, Qin J, Song F, Zeng W (2011) Iridovirus infection in Chinese Giant Salamanders, China, 2010. Emerging Infect Dis 17:2388–2389. doi:10.3201/eid1712.101758
16. Jiang YL, Zhang W, Jing HL, Gao LY (2011) Isolation and characterization of an Iridovirus from sick Giant salamander (*Andrias davidianus*). Chin J virol 27:274–282
17. Fijan N, Sulimanovic D, Bearzotti M, Muzinic D, Zwillenberg LO, Chilmonczyk M, Vautherot JF, Kinkelin PD (1983) Some properties of the *epithelioma papulosum cyprini* (EPC) cell line from carp cyprinus carpio. Ann Virol (Inst. Pasteur) 134E:207–220. doi:10.1016/j.bbr.2011.03.031
18. Reed LJ, Muench H (1938) A simple method of estimating fifty percent endpoints. Am J Hyg 27:493–497
19. Hoshino K, Isawa H, Tsuda Y, Yano K, Sasaki T, Yuda M, Takasaki T, Kobayashi M, Sawabe K (2007) Genetic characterization of a new insect flavivirus isolated from *Culex pipiens* mosquito in Japan. Virology 359:405–414. doi:10.1016/j.virol.2006.09.039
20. Daszak P, Berger L, Cunningham AA, Hyatt AD, Green E, Speare R (1999) Emerging infectious diseases and amphibian population declines. Emerg Infect Dis 5:735–748
21. Duffus AL, Pauli BD, Wozney K, Brunetti CR, Berrill M (2008) Frog virus 3-like infections in aquatic amphibian communities. J Wildl Dis 44:109–120

22. Gray MJ, Miller DL, Hoverman JT (2009) Ecology and pathology of amphibian ranaviruses. Dis Aquat Org 87:243–266. doi:10.3354/dao02138
23. Roberr J, Abramowitz L, Gantress J, Morales HD (2007) *Xenopus laevis*, a possible vector of ranavirus infection? J Wildl Dis 43:645–652
24. Schock DM, Bollinger TK, Collins JP (2009) Mortality rates differ among Amphibian populations exposed to three strains of a lethal Ranavirus. Eco Health 6:438–448. doi:10.1007/s10393-010-0279-0
25. Kik M, Martel A, Sluijs AS, Pasmans F, Wohlsein P, Grone A, Rijks JM (2011) Ranavirus-associated mass mortality in wild amphibians, The Netherlands, 2010, a first report. Vet J 190:284–286. doi:10.1006/viro.2001.1245
26. Baslserio A, Dalton KP, Cerro DA, Márquez I, Parra F, Prieto JM, Casais R (2010) Outbreak of common midwife toad virus in alpine newts (*Mesotriton alpestris cyreni*) and common midwife toads (*Alytes obstetricans*) in Northern Spain. A comparative pathological study of an emerging ranavirus. Vet J 186:256–258. doi:10.1016/j.tvjl.2009.07.038
27. Pessier AP (2002) An overview of amphibian skin disease. Semin Avian Exot Pet 11:162–174
28. Cunningham AA, Langton TE, Bennett PM, Drury SE, Gough RE, Macgregor SK (1996) Pathological and microbiological findings from incidents of unusual mortality of the common frog (*Rana temporaria*). Philos Trans R Soc Lond B Biol Sci 351:1539–1557. doi:10.1098/rstb.1996.0140
29. Jancovich JK, Davidson EW, Morado JF, Jacobs BL, Cliilins JP (1997) Isolation of a lethal virus from the endangered tiger salamander *Ambystoma tigdnum stebbinsi*. Dis Aquat Org 31:161–167
30. Plumb JA (2001) Disease recognition and diagnosis of fish. In: Coimbra J (ed) Modern aquaculture in the coastal zone. IOS Press, Amsterdam, pp 145–154
31. Miller DL, Gray MJ (2010) Amphibian decline and mass mortality, the value of visualizing ranavirus in tissue sections. Vet J 186:133–134. doi:10.1016/j.tvjl.2009.08.031
32. Goorha R (1982) Frog virus 3 DNA replication occurs in two stages. J Virol 43:519–528
33. Tidona CA, Schnitzler P, Kehm R, Darai G (1998) Is the major capsid protein of iridoviruses a suitable target for the study of viral evolution? Virus Genes 16:59–66. doi:10.1023/A:1007949710031
34. Webby R, Kalmakoff J (1998) Sequence comparison of the major capsid protein gene from 18 diverse iridoviruses. Arch Virol 143:1949–1966
35. Ward CW (1993) Progress towards a higher taxonomy of viruses. Res Virol (Institute Pasteur) 144:419–453